JOURNAL OF SOLID STATE CHEMISTRY 120, 187–196 (1995)

# Crystal Structures of $Li_4ZrF_8$ and $Li_3Zr_4F_{19}$ and Reinvestigation of the LiF-$ZrF_4$ Phase Diagram

Pierre Dugat, Malika El-Ghozzi, Jacques Metin, and Daniel Avignant

*Université Blaise Pascal, Laboratoire de Chimie des Solides, URA CNRS 444, 63177 Aubière, France*

Received October 18, 1994; in revised form August 4, 1995; accepted August 8, 1995

**The crystal structure of $Li_4ZrF_8$ has been refined from X-ray powder data using the Rietveld profile analysis. This compound is isostructural with $Li_4UF_8$ and crystallizes in the orthorhomic system (space group *Pnma*, no. 62) with cell parameters $a = 9.581(1)$ Å, $b = 9.611(1)$ Å, $c = 5.663(1)$ Å, $Z = 4$. The crystal structure of $Li_3Zr_4F_{19}$ has been solved from single-crystal X-ray diffraction data and refined to a conventional $R = 0.028$ ($R_w = 0.032$) for 4078 unique reflections with $I > 3\sigma(I)$. This fluoride crystallizes in the triclinic system ($P\bar{1}$ space group no. 2) with unit cell dimensions $a = 5.418(2)$ Å, $b = 10.822(2)$ Å, $c = 12.708(2)$ Å, $\alpha = 107.7°(1)$, $\beta = 92.0°(1)$, $\gamma = 103.4°(1)$. The 3D structure is built of corner- and edge-shared pentagonal bipyramids [$ZrF_7$]. This three-dimensional framework delimits channels parallel to the *a* direction, with an S-like shape, within which lie the $Li^+$ ions in octahedral coordination. These $(LiF_6)^{5-}$ octahedra are linked by corners or edges in hexameric units. Since a controversial statement about the LiF–$ZrF_4$ system exists in the literature, these published inconsistencies prompt a reinvestigation of the system. In the light of our structural studies a revised phase diagram of this system is presented.** © 1995 Academic Press, Inc.

## INTRODUCTION

Due to their potentialities for use in molten-salt technology and as nuclear reactor fuel solvent in chemical reprocessing of spent reactor fuel elements, combinations from the LiF–NaF–$ZrF_4$ ternary system have been extensively studied (1). In particular the LiF–$ZrF_4$ system has been the subject of several investigations (1, 2). More recently a new interest for these zirconium-based fluorinated materials has been provided by their potential use in glassy form as solid electrolytes for lithium batteries (3) or as IR transparent optical components for ultra-low loss optical fiber elaboration (4–7). Optimizing the performances of these glasses requires control of their compositions and therefore a good knowledge of the systems in which they are likely to recrystallize. However results of the above-mentioned investigations of the LiF–$ZrF_4$ system exhibit some discrepancies concerning the existence of $Li_4ZrF_8$, $Li_3Zr_4F_{19}$, and indeed $LiZr_4F_{17}$ phases. So a new investigation of this system by DTA and X-ray diffraction has been undertaken. The crystal structures of both $Li_4ZrF_8$ and $Li_3Zr_4F_{19}$ compounds have been solved and are reported in this paper as well as a new interpretation of the phase equilibrium diagram of this system in the light of these new crystallographic results.

## EXPERIMENTAL

Polycrystalline samples were prepared by reacting stoichiometric quantities of LiF (Merck, selectipur) and $ZrF_4$ in platinum tubes sealed under dry argon atmosphere. The zirconium tetrafluoride was prepared by direct fluorination of pure $ZrO_2$ (reagent grade) by heating it twice, in $F_2$ gas, overnight at 500°C.

X-ray powder patterns were recorded with a Siemens D500 diffractometer equipped with a high-intensity copper source and with a monochromator ($\lambda$ Cu$K\alpha_1$ = 1.5405 Å) located in the diffracted beam. The sample used for the structure refinement of $Li_4ZrF_8$ was passed through a 80-$\mu$m sieve before the filling of the sample holder. During data collection, the sample holder was rotating at the speed of 30 revolutions per minute.

DTA experiments were carried out under dry argon gas flow using a Netzsch thermal analyzer equipped with a 1550°C DDK probe. The phase equilibrium diagram, the main characteristics of which are presented in Table 1, was established by DTA experiments from the heating curves of samples annealed at suitable temperatures. A heating rate of 300°C/h, was used in these experiments, which were carried out in platinum crucibles. For the high LiF content part of the diagram no subsequent mass loss was observed at the end of each heating period. For the high $ZrF_4$ content part of the diagram, the use of a sealed platinum tube avoided the mass loss and allowed verification that there is no invariant stretch at temperatures higher than 580°C. In the sample preparation, the equilibrium was assumed to have been achieved when X-ray powder patterns showed no change after repeated heat treatments of a specimen



0022-4596/95 $12.00

**TABLE 1**
**Main Characteristics of the LiF–$ZrF_4$ Phase Diagram**

| Compositions (mole% $ZrF_4$) | Invariant temperatures (°C) | Type of invariant | Phase reaction on cooling |
|---|---|---|---|
| 0 | 845 | Congruent m.p. | $L \rightarrow LiF$ |
| 16 | 608 | Eutectic | $L + LiF \rightarrow Li_3ZrF_7$ |
| 20 | 500 | Decomposition | $Li_4ZrF_8 \rightarrow LiF + Li_3ZrF_7$ |
| 25 | 656 | Congruent m.p. | $L \rightarrow Li_3ZrF_7$ |
| | 495 | Decomposition | $2Li_3ZrF_7 \rightarrow Li_2ZrF_6 + Li_4ZrF_8$ |
| 31 | 598 | Eutectic | $L \rightarrow Li_3ZrF_7 + Li_2ZrF_6$ |
| 33 | 602 | Congruent m.p. | $L \rightarrow Li_2ZrF_6$ |
| 50 | 500 | Eutectic | $L \rightarrow Li_2ZrF_6 + Li_3Zr_4F_{19}$ |
| 55 | 510 | Peritectic | $L + ZrF_4 \rightarrow Li_3Zr_4F_{19}$ |
| 57.1 | 472 | Decomposition | $2Li_3Zr_4F_{19} \rightarrow 3Li_2ZrF_6 + 5ZrF_4$ |
| 60 | 580 | Phase transition | $\alpha\text{-}ZrF_4 \rightarrow \beta\text{-}ZrF_4$ |
| 100 | Sub. | | |

or when the data were consistent with the results from a previous set of experiments.

## CRYSTAL STRUCTURE REFINEMENT OF $Li_4ZrF_8$

From comparison of their X-ray powder patterns and consecutively from their crystal chemical characteristics it has been established in a preceeding work that $Li_4ZrF_8$ and $Li_4UF_8$ are two isostructural phases (8). So the refinement of the crystal structure of $Li_4ZrF_8$ was performed using the Rietveld method and the $Li_4UF_8$ structure (9) as starting model. However as polycrystalline samples of $Li_4ZrF_8$ always contain traces of $Li_2ZrF_6$, which will become perfectly understandable when we consider the redrawn phase diagram (see Fig. 5), this second phase was taken into account in the refinement. The data reported by Brunton (10) served as a structural model in the refinement procedure.

After some cycles, the refinement converged to conventional Rietveld reliability factors (%), $R_i = 5.74$, $R_p = 11.48$, $R_{wp} = 13.06$, and $R_{exp} = 3.35$. It can be noted that the isotropic temperature factors of the lithium atoms were fixed at 0.3 as one of them tends to become negative whereas the other simultaneously increases. This is often observed when the contrast between the scattering power of atoms is large and is partly due to the correlation of thermal parameters for light atoms with the background level. Of course, these values have no physical meaning

**TABLE 2**
**Structure and Profile Parameters of the Rietveld Refinement of $Li_4ZrF_8$ Containing $Li_2ZrF_6$ (X-Ray Powder Pattern Recorded at 298 K)**

Scan
$2\theta$ range (°): 10–110; step scan (°), 0.02; time/step (s), 30.
Number of reflections: 826
Number of parameters: 58
Zero point (°): 0.006(2)

**$Li_4ZrF_8$**
Cell parameters: $a = 9.581(1)$ Å, $b = 9.611(1)$ Å, $c = 5.663(1)$ Å
Cell volume: $V = 521.5(1)$ Å$^3$, $Z = 4$
Space group: *Pnma* (no. 62)
Profile parameters: $U_1 = -0.423(3)$, $V_1 = 0.579(4)$, $W_1 = 0.028(3)$, $U_2 = 4.41(3)$, $V_2 = -5.11(1)$, $W_2 = 3.16(5)$, $C = 0.0226(5)$, $D = -1.098(3)$

**$Li_2ZrF_6$**
Cell parameters: $a = 4.974(8)$ Å, $c = 4.655(4)$ Å
Cell volume: $V = 99.7(4)$ Å$^3$, $Z = 1$
Space group: *P3ml* (no. 164)
Profile parameters: $U_1 = -0.0044(5)$, $V_1 = 0.200(2)$, $W_1 = 0.0281(3)$, $U_2 = 2.00(6)$, $V_2 = -3.30(3)$, $W_2 = 3.21(9)$, $C = -0.209(6)$, $D = 0.556(2)$
Reliability factors (%): $R_i = 5.74$, $R_p = 11.48$, $R_{wp} = 13.06$, $R_{exp} = 3.35$

**TABLE 3**
**Positional Parameters and Isotropic Thermal Parameters for $Li_4ZrF_8$**

| Atoms | Sites | $x$ | $y$ | $z$ | $B$ (Å$^2$) |
|---|---|---|---|---|---|
| Li(1) | 8d | 0.370(2) | 0.063(1) | 0.088(3) | 0.3[a] |
| Li(2) | 8d | 0.390(1) | 0.071(1) | 0.597(3) | 0.3[a] |
| Zr | 4c | 0.1348(2) | 1/4 | 0.3718(4) | 2.07(3) |
| F(1) | 8d | 0.021(1) | 0.118(1) | 0.158(3) | 1.8(2) |
| F(2) | 8d | 0.030(1) | 0.121(1) | 0.603(3) | 2.6(2) |
| F(3) | 8d | 0.237(1) | 0.463(1) | 0.378(2) | 2.4(1) |
| F(4) | 4c | 0.287(1) | 1/4 | 0.114(5) | 2.5(2) |
| F(5) | 4c | 0.295(1) | 1/4 | 0.615(4) | 2.3(2) |

[a] Fixed value.

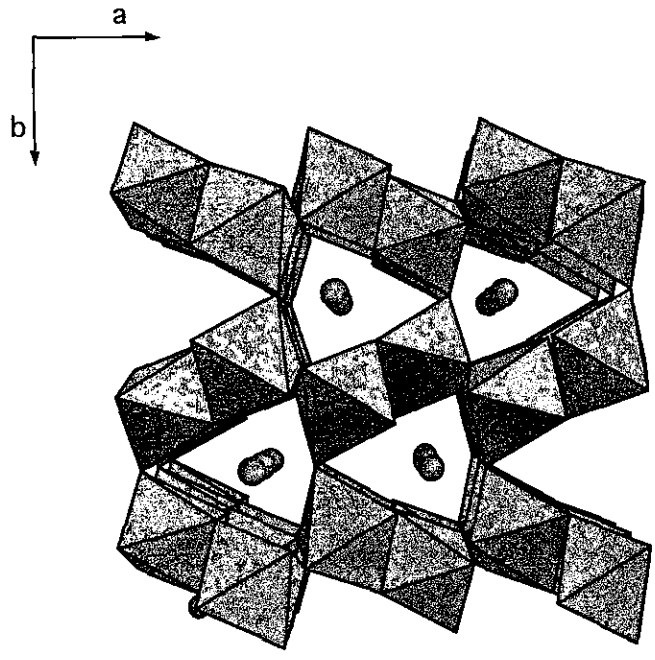


FIG. 1. Perspective view of the structure of $Li_4ZrF_8$ projected on the (0 0 1) plane.

but can be considered as acceptable within the general 3 e.s.d.

The conditions of data collection and profile refinements are gathered in Table 2. The observed and calculated patterns are shown in Fig. 2. The final atomic coordinates and thermal parameters are given in Table 3. The main interatomic distances and angles are presented in Table 4.

Figure 1 represents a projection of the structure of $Li_4ZrF_8$ along the [001] direction. The structure is built of double octahedral chains of lithium which are join by vertex- and edge-sharing to form a three-dimensional framework. This framework delimits tunels running along the $c$ direction within which the $Zr^{4+}$ ions in eightfold coordination essential to the stability of the structure alternate with vacancies.

## CRYSTAL STRUCTURE DETERMINATION AND REFINEMENT OF $Li_3Zr_4F_{19}$

By centering on 25 reflections followed by a least-squares refinement of the measured setting angles a triclinic cell with dimensions $a$ = 5.418(2) Å, $b$ = 10.822(2) Å, $c$ = 12.708(2) Å, $\alpha$ = 107.7°(1), $\beta$ = 92.0°(1), $\gamma$ = 103.4°(1) was obtained. Intensities were recorded with an automatic four-circle Nonius CAD4 diffractometer under the conditions mentioned in Table 5.

The structure was solved from the Patterson function. Refinement of all Zr coordinates deduced from this function, in the centric $P\bar{1}$ space group, with individual isotropic thermal parameters results in $R$ = 0.132.

Then successive Fourier syntheses revealed the fluorine positions. After a few cycles of refinement a difference Fourier synthesis allowed us to locate the Li atoms. Subsequent full-matrix least-squares refinements in which all atoms were assigned anisotropic thermal parameters led

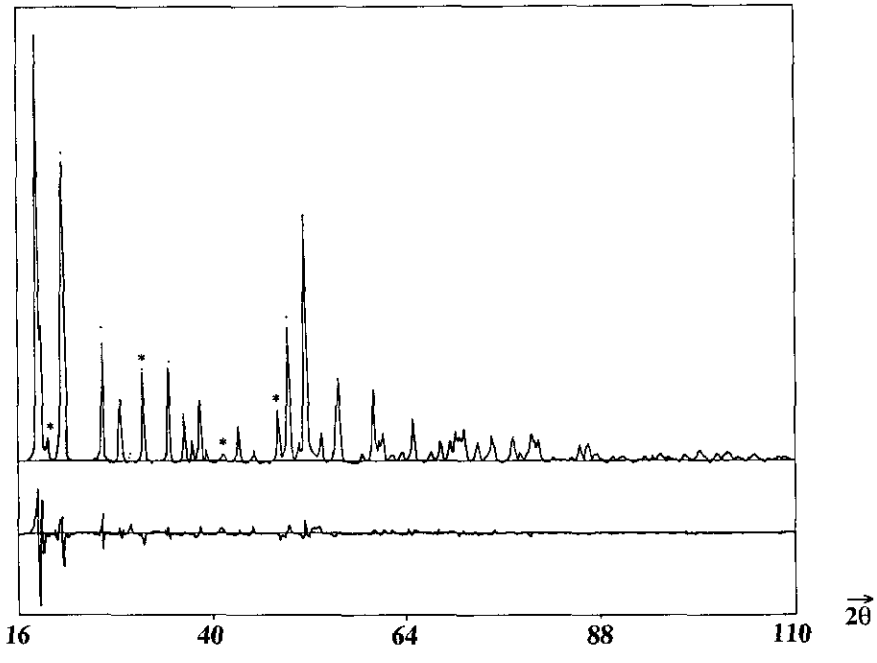


FIG. 2. Observed and calculated X-ray powder patterns of $Li_4ZrF_8$ and difference function. Asterisks indicate diffraction peaks relative to $Li_2ZrF_6$.

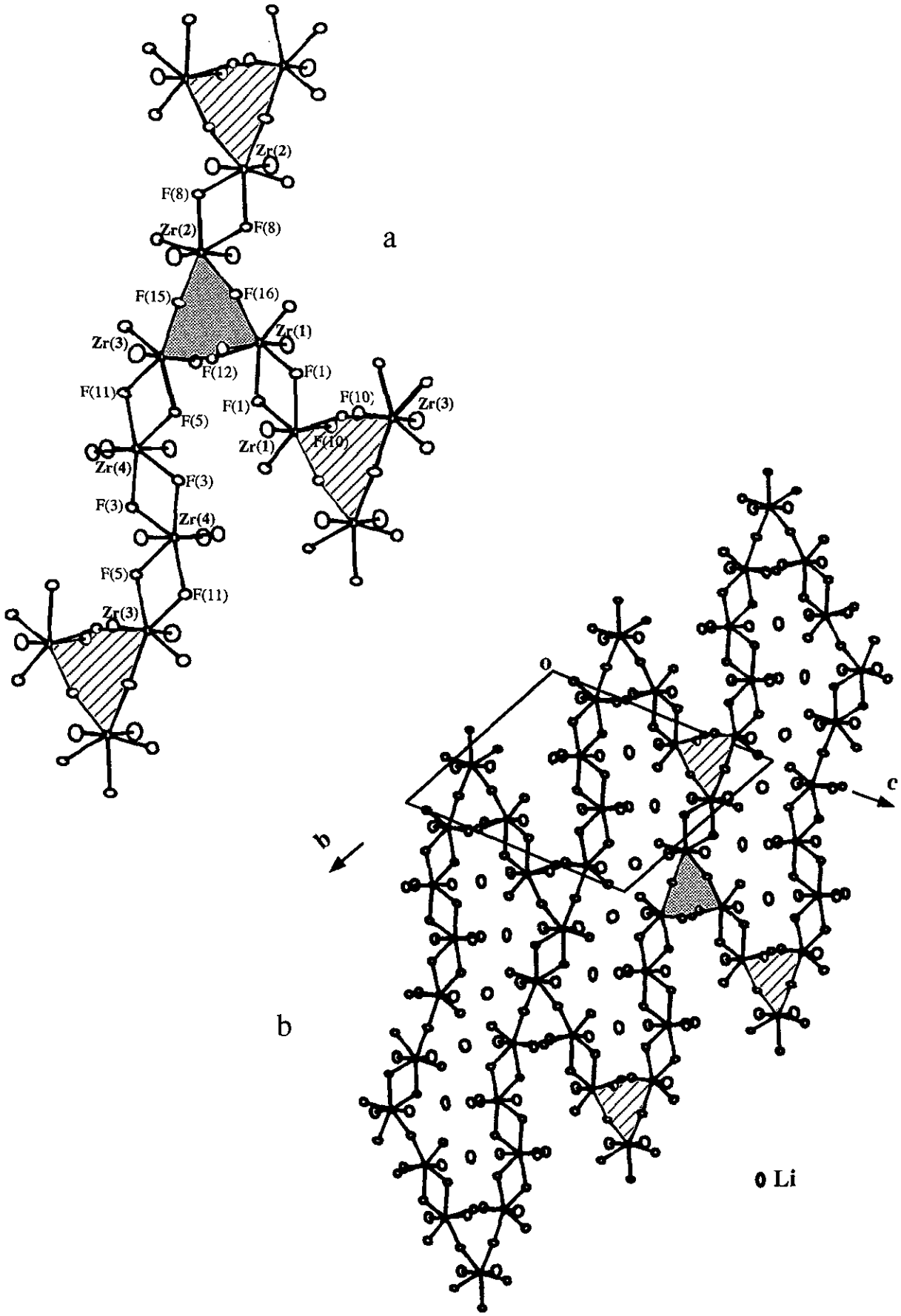


FIG. 3. Projection of the structure of $Li_3Zr_4F_{19}$ on the (1 0 0) plane. (a) Detail of the basal structural unit; (b) view of the structure as a whole.

TABLE 4
Selected Distances (Å) and Angles (°) in $Li_4ZrF_8$

| | | | | Zr polyhedron [8] | | | | |
|---|---|---|---|---|---|---|---|---|
| **Zr** | **F(2)** | **F(2)** | **F(4)** | **F(5)** | **F(1)** | **F(1)** | **F(3)** | **F(3)** |
| **F(2)** | **2.06(1)** | 2.48(1) | 3.91(2) | 2.83(1) | 2.52(2) | 3.56(2) | 4.04(1) | 2.49(1) |
| **F(2)** | 73.9(4) | **2.06(1)** | 3.91(2) | 2.83(1) | 3.56(2) | 2.52(2) | 2.49(1) | 4.04(1) |
| **F(4)** | 142.4(2) | 142.4(2) | **2.06(2)** | 2.84(4) | 2.86(1) | 2.86(1) | 2.58(2) | 2.58(2) |
| **F(5)** | 86.5(5) | 86.5(5) | 86.9(8) | **2.06(2)** | 3.90(2) | 3.90(2) | 2.51(2) | 2.51(2) |
| **F(1)** | 75.2(5) | 118.9(3) | 87.7(5) | 141.6(2) | **2.07(1)** | 2.54(1) | 4.10(1) | 2.53(1) |
| **F(1)** | 118.9(3) | 75.2(5) | 87.7(5) | 141.6(2) | 75.9(3) | **2.07(1)** | 2.53(1) | 4.10(1) |
| **F(3)** | 137.8(5) | 69.9(3) | 73.0(3) | 70.7(3) | 142.4(4) | 71.4(3) | **2.27(1)** | 4.09(1) |
| **F(3)** | 69.9(3) | 137.8(5) | 73.0(3) | 70.7(3) | 71.4(3) | 142.4(4) | 129.0(2) | **2.27(1)** |
| | | | | ⟨Zr–F⟩ =. 2.11 | | | | |

| | | | Li(1) polyhedra [6] | | | |
|---|---|---|---|---|---|---|
| **Li(1)** | **F(3)** | **F(2)** | **F(4)** | **F(2)** | **F(3)** | **F(1)** |
| **F(3)** | **1.84(2)** | 2.97(1) | 3.07(1) | 2.49(1) | 2.93(2) | 3.90(2) |
| **F(2)** | 103.2(9) | **1.96(2)** | 2.91(2) | 2.66(1) | 4.00(2) | 2.52(2) |
| **F(4)** | 107.7(11) | 95.6(8) | **1.97(2)** | 3.97(1) | 2.58(2) | 2.88(2) |
| **F(2)** | 80.4(7) | 84.3(8) | 171.7(13) | **2.01(2)** | 3.12(1) | 2.71(1) |
| **F(3)** | 96.1(9) | 160.7(11) | 78.7(9) | 98.7(8) | **2.10(2)** | 2.84(1) |
| **F(1)** | 162.4(11) | 76.6(9) | 89.8(8) | 82.1(8) | 84.9(7) | **2.11(2)** |
| | | | ⟨Li(1)–F⟩ = 2.00 | | | |

| | | | Li(2) polyhedron [6] | | | |
|---|---|---|---|---|---|---|
| **Li(2)** | **F(3)** | **F(5)** | **F(1)** | **F(1)** | **F(2)** | **F(3)** |
| **F(3)** | **1.95(2)** | 2.51(2) | 2.84(1) | 3.18(1) | 4.15(2) | 2.93(2) |
| **F(5)** | 80.1(7) | **1.95(1)** | 2.95(2) | 3.96(1) | 3.02(2) | 3.15(1) |
| **F(1)** | 92.9(9) | 97.6(9) | **1.97(2)** | 2.91(1) | 3.15(2) | 4.19(1) |
| **F(1)** | 106.1(7) | 166.9(11) | 93.6(7) | **2.03(1)** | 2.71(1) | 2.53(1) |
| **F(2)** | 168.2(9) | 92.8(8) | 97.4(7) | 79.1(6) | **2.22(2)** | 2.97(1) |
| **F(3)** | 88.1(6) | 96.8(8) | 165.6(7) | 72.3(6) | 83.4(7) | **2.25(2)** |
| | | | ⟨Li(2)–F⟩ = 2.06 | | | |

to the final value $R = 0.028$ ($R_w = 0.032$). The bond length–bond strength analysis of the structure performed at this stage using Brese and O'Keefe's method (11) confirms the lithium position assignments (see Table 8).

The scattering factors for $Zr^{4+}$, $F^-$, and $Li^+$, as well as the anomalous dispersion terms for the Mo$K\alpha$ radiation, were taken from the "International Tables for X-ray Crystallography" (12). All computer programs used for data collection, reduction and refinement, details of which are given in Table 5, were from the CAD4 SDP Package (13).

Final positional and thermal parameters are given in

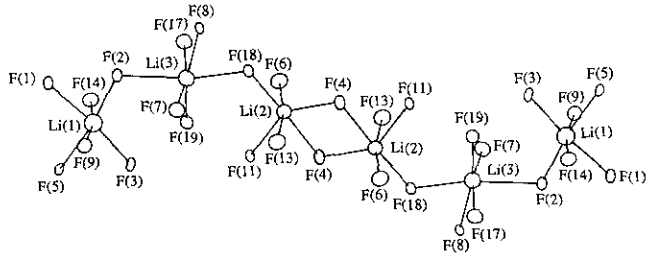


FIG. 4. String of six Li octahedra.

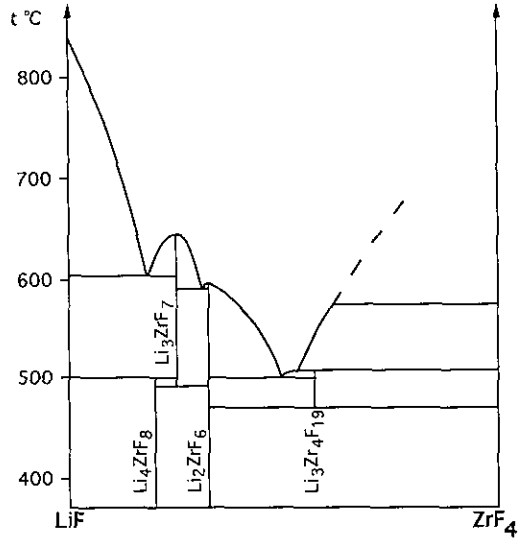


FIG. 5. Phase equilibrium diagram of the $LiF–ZrF_4$ system.

TABLE 5
Crystal Data, Data Collection and Refinement Details for $Li_3Zr_4F_{19}$

| | |
|---|---|
| Formula | $Li_3Zr_4F_{19}$ |
| $F_w$ (g) | 746.66 |
| Symmetry | Triclinic ($P\bar{1}$, no. 2) |
| Unit cell parameters | $a$ = 5.418(2) Å<br>$b$ = 10.822(2) Å<br>$c$ = 12.708(2) Å<br>$\alpha$ = 107.7(1)°<br>$\beta$ = 92.0(1)°<br>$\gamma$ = 103.4(2)° |
| $V$ (Å$^3$) | 685.8(3) |
| $Z$ | 2 |
| $D_c$ (g cm$^{-3}$) | 3.62 |
| Data collection temperature (K) | 294 |
| Crystal volume (mm$^3$) | 0.13 × 0.16 × 0.35 |
| Radiation | Mo$K\alpha$ ($\lambda$ = 0.71069 Å); graphite monochromated |
| Linear absorption coefficient (cm$^{-1}$) | 31.5 |
| Transmission factors | 0.86–0.99[a] |
| Scan mode | $\omega$–2$\theta$ |
| Scan width | (0.85 + 0.35 tan $\theta$)° |
| Scan aperture | (2.70 + 1.00 tan $\theta$) (mm) |
| 2$\theta$ limits (°) | 2.0 ≤ 2$\theta$ ≤ 70.00 |
| Data collected | $\bar{8} \le h \le 8$, $\bar{17} \le k \le 17$, $0 \le l \le 20$ |
| Period of intensity control | 3600 sec, $\sigma$ = 0.02 |
| Number of measured reflections | 6040 |
| Number of unique data | 4079 ($I > 3\sigma(I)$) |
| $p$ factor | 0.04 |
| Final number of variables | 236 |
| Secondary extinction coefficient | 5.82(6) × 10$^{-7}$ |
| $R$ | 0.028 |
| $R_w$ | 0.032 |
| Error of an observation of unit weight | 0.825 |
| Shift to e.s.d. | 0.00 |
| Max. and min. electron density in final Fourier difference map | 0.83, −0.87 $e$ Å$^{-3}$ |

[a] An empirical absorption correction was applied.

Table 6. The main interatomic distances are mentioned in Table 7. A list of the observed and calculated structure factors may be obtained from the authors, on request.

## DESCRIPTION OF THE STRUCTURE AND DISCUSSION

This structure may be described from a structural unit built of three pentagonal bipyramids [$ZrF_7$] involving Zr(1), Zr(2), and Zr(3) and linked in a triangle by sharing one corner, namely, F(16), F(15), and F(12), between Zr(1) and Zr(2), Zr(2) and Zr(3), and Zr(1) and Zr(3), respectively (Fig. 3a). These groups of three [$ZrF_7$] polyhedra are further linked to three other identical groups to form a corrugated polyhedral layer by sharing edges in two ways:

- directly for both [Zr(1)$F_7$] and [Zr(2)$F_7$] polyhedra linked, respectively, to [Zr(1)$F_7$] and [Zr(2)$F_7$] polyhedra belonging to two different adjacent structural units through F(1)–F(1) and F(8)–F(8) edges.
- through a binuclear unit built of two [Zr(4)$F_7$] polyhedra sharing a F(3)–F(3) edge for the third [Zr(2)$F_7$] polyhedron which shares a F(5)–F(11) edge with this binuclear entity. Then the corrugated polyhedral layers extending parallel to the ($\bar{1}\bar{1}2$) plane are joined together by sharing F(10) corners. More accurately, each [Zr(1)$F_7$] polyhedron of one layer is linked through a F(10) vertex to one [Zr(3)$F_7$] polyhedron of an adjacent layer. This three-dimensional framework of corner- and edge-shared pentagonal bipyramids delimits channels with an S-like shape running along the [100] direction, within which lie the $Li^+$ ions gathered together in hexameric units of octahedra (Fig. 3b). These Li octahedra strings are built up from two units of three corner-shared octahedra involving Li(1), Li(3), and Li(2) related by a center of symmetry and held together through a common F(4)–F(4) edge shared between the two [Li(2)$F_6$] octahedra (Fig. 4).

The [Li(3)$F_6$] octahedron is strongly distorted with the shortest and the longest Li–F distances, namely 1.89 and 2.36 Å. But despite this strong distortion the mean Li–F distances within all the [$LiF_6$] octahedra, namely 2.10, 2.09, and 2.10 in [Li(1)$F_6$], [Li(2)$F_6$], and [Li(3)$F_6$] are in good agreement with the Shannon distance of 2.07 Å.

The [$LiF_6$] octahedra strings are further linked to the three-dimensional framework of corner- and edge-shared pentagonal bipyramids [$ZrF_7$] by sharing corners and edges in such a way that:

- each [Li(1)$F_6$] octahedron shares an edge F(1)–F(2) with one [Zr(1)$F_7$] pentagonal bipyramid and a corner F(1) with an other [Zr(1)$F_7$] polyhedron of one layer called I, as well as one corner F(14) with one [Zr(1)$F_7$] bipyramid of the next layer called II and an edge F(3)–F(5) and a corner F(9) with two [Zr(4)$F_7$] polyhedra. The [Li(2)$F_6$] octahedra share an edge F(4)–F(11) with a [Zr(3)$F_7$] and two corners F(4) and F(6) with [Zr(3)$F_7$] and [Zr(2)$F_7$] of layer II and two corners F(13) and F(18) with [Zr(3)$F_7$] and [Zr(2)$F_7$] of layer I. The [Li(3)$F_6$] octahedra are linked by edge and corner sharing involving F(8)–F(18) and F(2) to [Zr(2)$F_7$] and [Zr(1)$F_7$] pentagonal bipyramids of layer I and by sharing a corner F(17) with one [Zr(2)$F_7$] polyhedron of layer II as well as to two different [Zr(4)$F_7$] polyhedra by sharing corners F(7) and F(19).

## PHASE EQUILIBRIA IN THE LiF–$ZrF_4$ SYSTEM

In their pioneering work on the LiF–$ZrF_4$ system, Thoma *et al.* (1) showed the existence of complex fluorides with LiF : $ZrF_4$ ratios of 3 : 1, 2 : 1, and 3 : 4 and reported a polymorphic transition for the metastable $Li_3ZrF_7$ com-

**TABLE 6**
**Positional Parameters and Isotropic Thermal Parameters for $Li_3Zr_4F_{19}$**

| Atoms | Sites | $x$ | $y$ | $z$ | $B_{iso}$ or $B_{eq}$ |
|---|---|---|---|---|---|
| Zr(1) | 2i | 0.33371(6) | 0.87713(3) | 0.36924(3) | 0.547(5) |
| Zr(2) | 2i | 0.06152(6) | 0.33804(3) | 0.94659(3) | 0.626(5) |
| Zr(3) | 2i | 0.09931(6) | 0.94827(3) | 0.79185(3) | 0.557(5) |
| Zr(4) | 2i | 0.13795(6) | 0.61669(3) | 0.63427(3) | 0.672(5) |
| Li(1) | 2i | 0.716(2) | 0.738(1) | 0.489(1) | 2.2(2) |
| Li(2) | 2i | 0.524(2) | 0.835(1) | 0.940(1) | 2.5(2) |
| Li(3) | 2i | 0.586(2) | 0.489(1) | 0.791(1) | 2.2(4) |
| F(1) | 2i | 0.3742(5) | 0.0694(2) | 0.4947(2) | 1.38(4) |
| F(2) | 2i | 0.5082(5) | 0.2752(2) | 0.6547(2) | 1.39(4) |
| F(3) | 2i | 0.8722(5) | 0.5709(2) | 0.4872(2) | 1.28(4) |
| F(4) | 2i | 0.6613(6) | 0.0006(3) | 0.0741(2) | 2.05(5) |
| F(5) | 2i | 0.9662(5) | 0.7827(2) | 0.6447(2) | 1.17(4) |
| F(6) | 2i | 0.2439(6) | 0.7463(3) | −0.0024(3) | 2.26(5) |
| F(7) | 2i | 0.1486(6) | 0.4586(3) | 0.2965(3) | 2.10(5) |
| F(8) | 2i | 0.8739(5) | 0.4800(2) | 0.9174(2) | 1.33(4) |
| F(9) | 2i | 0.4152(5) | 0.6993(3) | 0.5602(2) | 1.72(5) |
| F(10) | 2i | 0.6120(5) | 0.9813(3) | 0.2967(2) | 1.59(4) |
| F(11) | 2i | 0.7355(5) | 0.2163(2) | 0.2186(2) | 1.47(4) |
| F(12) | 2i | 0.1195(5) | 0.9871(2) | 0.3106(2) | 1.44(4) |
| F(13) | 2i | 0.2013(6) | 0.1114(3) | 0.1441(3) | 2.26(6) |
| F(14) | 2i | 0.9553(5) | 0.1906(3) | 0.5620(2) | 1.72(5) |
| F(15) | 2i | 0.1225(6) | 0.1480(3) | 0.8744(3) | 2.26(5) |
| F(16) | 2i | 0.1693(5) | 0.7541(2) | 0.2135(2) | 1.60(4) |
| F(17) | 2i | 0.3358(5) | 0.4087(3) | 0.8687(2) | 2.05(5) |
| F(18) | 2i | 0.2973(5) | 0.3220(2) | 0.0617(2) | 1.54(4) |
| F(19) | 2i | 0.3627(5) | 0.5486(3) | 0.7117(2) | 1.94(5) |

Anisotropic thermal parameters[a]

| Atoms | $U_{11}$ | $U_{22}$ | $U_{33}$ | $U_{12}$ | $U_{13}$ | $U_{23}$ |
|---|---|---|---|---|---|---|
| Zr(1) | 0.0073(1) | 0.0073(1) | 0.0066(1) | 0.0019(1) | 0.0010(1) | 0.0028(1) |
| Zr(2) | 0.0092(1) | 0.0070(1) | 0.0076(1) | 0.0024(1) | 0.0012(1) | 0.0020(1) |
| Zr(3) | 0.0076(1) | 0.0072(1) | 0.0072(1) | 0.0026(1) | 0.0017(1) | 0.0029(1) |
| Zr(4) | 0.0095(1) | 0.0077(1) | 0.0091(1) | 0.0029(1) | 0.0024(1) | 0.0030(1) |
| Li(1) | 0.018(3) | 0.036(3) | 0.036(3) | 0.003(3) | 0.011(3) | 0.022(3) |
| Li(2) | 0.026(3) | 0.041(4) | 0.033(4) | 0.011(3) | 0.018(3) | 0.016(3) |
| Li(3) | 0.020(3) | 0.040(3) | 0.032(3) | 0.004(3) | 0.007(3) | 0.026(2) |
| F(1) | 0.0212(9) | 0.0162(8) | 0.0143(9) | 0.0112(6) | −0.0038(8) | −0.0004(7) |
| F(2) | 0.0204(9) | 0.0152(8) | 0.018(1) | 0.0096(7) | −0.0009(8) | −0.0022(7) |
| F(3) | 0.0213(9) | 0.0114(7) | 0.0160(9) | 0.0089(6) | −0.0016(8) | 0.0013(7) |
| F(4) | 0.036(1) | 0.0209(9) | 0.019(1) | 0.0150(8) | −0.013(1) | −0.0006(8) |
| F(5) | 0.0198(9) | 0.0116(7) | 0.0135(9) | 0.0088(6) | −0.0035(8) | 0.0008(6) |
| F(6) | 0.020(1) | 0.034(1) | 0.034(1) | 0.001(1) | 0.012(1) | 0.0188(9) |
| F(7) | 0.021(1) | 0.032(1) | 0.026(1) | 0.003(1) | 0.0130(9) | 0.0185(8) |
| F(8) | 0.024(1) | 0.0116(7) | 0.0127(9) | 0.0092(7) | −0.0058(8) | −0.0015(7) |
| F(9) | 0.017(1) | 0.026(1) | 0.027(1) | 0.0044(8) | 0.0102(9) | 0.0146(8) |
| F(10) | 0.018(1) | 0.0224(9) | 0.0230(9) | 0.0013(8) | 0.0101(8) | 0.0129(7) |
| F(11) | 0.024(1) | 0.0164(8) | 0.0142(9) | 0.0110(7) | −0.0058(8) | −0.0005(7) |
| F(12) | 0.025(1) | 0.0163(8) | 0.0139(9) | 0.0114(7) | −0.0043(8) | 0.0023(7) |
| F913) | 0.021(1) | 0.038(1) | 0.029(1) | 0.006(1) | 0.0163(9) | 0.015(1) |
| F(14) | 0.0144(9) | 0.026(1) | 0.029(1) | 0.0022(8) | 0.0108(8) | 0.0155(8) |
| F(15) | 0.045(1) | 0.0160(8) | 0.022(1) | 0.0184(8) | −0.013(1) | −0.0041(8) |
| F(16) | 0.028(1) | 0.0150(8) | 0.015(1) | 0.0100(7) | −0.0081(9) | −0.0012(7) |
| F(17) | 0.022(1) | 0.029(1) | 0.030(1) | 0.002(1) | 0.0145(9) | 0.0162(8) |
| F(18) | 0.025(1) | 0.0192(8) | 0.016(1) | 0.0118(7) | −0.0045(8) | 0.0038(7) |
| F(19) | 0.025(1) | 0.0279(9) | 0.026(1) | 0.0141(8) | −0.0032(9) | 0.0103(8) |

[a] The form of the anisotropic displacement parameters is $\exp[-2\pi^2(h^2a^{*2}U_{11} + k^2b^{*2}U_{22} + l^2c^{*2}U_{33} + 2hka^*b^*U_{12} + 2hla^*c^*U_{13} + 2klb^*c^*U_{23})]$

TABLE 7
Main Interatomic Distances (Å) and Angles (°) in $Li_3Zr_{419}$

**Zr(1) polyhedron [7]**

| Zr(1) | F(14) | F(2) | F(16) | F(10) | F(12) | F(1) | F(1) |
|---|---|---|---|---|---|---|---|
| F(14) | **1.92(1)** | 2.94(1) | 2.88(1) | 3.99(1) | 2.84(1) | 3.09(1) | 2.82(1) |
| F(2) | 97.9(1) | **1.98(1)** | 2.52(1) | 2.96(1) | 3.96(1) | 2.45(1) | 3.85(1) |
| F(16) | 92.4(1) | 77.3(1) | **2.05(1)** | 2.90(1) | 2.53(1) | 4.05(1) | 4.02(1) |
| F(10) | 168.6(1) | 93.5(1) | 89.2(1) | **2.08(1)** | 2.69(1) | 2.87(1) | 2.87(1) |
| F(12) | 89.4(1) | 151.5(1) | 74.9(1) | 80.1(1) | **2.11(1)** | 3.91(1) | 2.47(1) |
| F(1) | 98.8(1) | 72.8(1) | 149.3(1) | 85.4(1) | 133.3(1) | **2.15(1)** | 2.28(1) |
| F(1) | 87.2(1) | 136.7(1) | 145.7(1) | 85.1(1) | 70.8(1) | 63.9(1). | **2.16(1)** |

⟨Zr(1) − F⟩ = 2.06 Å

**Zr(2) polyhedron [7]**

| Zr(2) | F(17) | F(6) | F(18) | F(15) | F(8) | F(8) | F(16) |
|---|---|---|---|---|---|---|---|
| F(17) | **1.95(1)** | 3.90(1) | 2.88(1) | 2.81(1) | 3.00(1) | 2.82(1) | 2.85(1) |
| F(6) | 171.3(1) | **1.96(1)** | 2.87(1) | 2.84(1) | 2.96(1) | 2.92(1) | 2.77(1) |
| F(18) | 94.1(1) | 93.2(1) | **1.98(1)** | 2.53(1) | 2.47(1) | 3.87(1) | 4.00(1) |
| F(15) | 88.2(1) | 88.8(1) | 76.7(1) | **2.09(1)** | 4.08(1) | 4.02(1) | 2.50(1) |
| F(8) | 94.3(1) | 92.4(1) | 73.8(1) | 150.5(1) | **2.13(1)** | 2.33(1) | 4.01(1) |
| F(8) | 87.1(1) | 90.5(1) | 139.8(1) | 143.0(1) | 66.1(1) | **2.14(1)** | 2.52(1) |
| F(16) | 87.4(1) | 83.9(1) | 148.4(1) | 71.8(1) | 137.6(1) | 71.7(1) | **2.17(1)** |

⟨Zr(2) − F⟩ = 2.06 Å

**Zr(3) polyhedron [7]**

| Zr(3) | F(13) | F(4) | F(15) | F(10) | F(12) | F(5) | F(11) |
|---|---|---|---|---|---|---|---|
| F(13) | **1.91(1)** | 2.89(1) | 2.88(1) | 3.99(1) | 2.83(1) | 2.85(1) | 3.07(1) |
| F(4) | 96.4(1) | **1.96(1)** | 2.42(1) | 2.92(1) | 3.89(1) | 3.81(1) | 2.43(1) |
| F(15) | 92.7(1) | 73.8(1) | **2.07(1)** | 2.84(1) | 2.49(1) | 4.01(1) | 4.02(1) |
| F(10) | 170.7(1) | 92.0(1) | 86.0(1) | **2.09(1)** | 2.73(1) | 2.88(1) | 2.95(1) |
| F(12) | 89.5(1) | 146.8(1) | 73.2(1) | 81.3(1) | **2.10(1)** | 2.54(1) | 3.98(1) |
| F(5) | 89.8(1) | 138.5(1) | 147.0(1) | 86.3(1) | 73.9(1) | **2.12(1)** | 2.33(1) |
| F(11) | 98.0(1) | 72.4(1) | 145.5(1) | 88.2(1) | 139.2(1) | 66.2(1) | **2.14(1)** |

⟨Zr(3) − F⟩ = 2.06 Å

**Zr(4) polyhedron [7]**

| Zr(4) | F(19) | F(7) | F(9) | F(11) | F(3) | F(3) | F(5) |
|---|---|---|---|---|---|---|---|
| F(19) | **1.94(1)** | 2.75(1) | 2.86(1) | 2.61(1) | 2.59(1) | 3.93(1) | 3.93(1) |
| F(7) | 90.0(1) | **1.95(1)** | 3.93(1) | 2.90(1) | 2.98(1) | 2.87(1) | 2.87(1) |
| F(9) | 93.6(1) | 176.3(1) | **1.98(1)** | 2.89(1) | 2.84(1) | 2.93(1) | 2.91(1) |
| F(11) | 79.9(1) | 90.7(1) | 89.4(1) | **2.12(1)** | 4.18(1) | 3.97(1) | 2.33(1) |
| F(3) | 78.8(1) | 93.9(1) | 87.4(1) | 158.2(1) | **2.13(1)** | 2.37(1) | 4.00(1) |
| F(3) | 145.4(1) | 87.9(1) | 89.5(1) | 134.7(1) | 66.9(1) | **2.17(1)** | 2.47(1) |
| F(5) | 145.2(1) | 87.9(1) | 88.8(1) | 65.5(1) | 136.0(1) | 69.2(1) | **2.18(1)** |

⟨Zr(4) − F⟩ = 2.07 Å

**Li(1) polyhedra [6]**

| Li(1) | F(9) | F(14) | F(2) | F(3) | F(1) | F(5) |
|---|---|---|---|---|---|---|
| F(9) | **1.91(1)** | 3.88(1) | 2.86(1) | 3.15(1) | 2.80(1) | 2.97(1) |
| F(14) | 169.8(5) | **1.98(1)** | 3.00(1) | 2.80(1) | 2.91(1) | 2.77(1) |
| F(2) | 90.7(4) | 94.5(4)) | **2.11(1)** | 3.67(1) | 2.45(1) | 4.31(1) |
| F(3) | 100.7(5) | 84.7(4) | 118.2(5) | **2.17(1)** | 4.35(1) | 2.47(1) |
| F(1) | 85.6(4) | 87.9(4) | 69.5(3) | 169.7(4) | **2.20(1)** | 3.46(1) |
| F(5) | 91.6(4) | 82.2(2) | 172.2(3) | 68.7(3) | 103.3(3) | **2.22(1)** |

⟨Li(1) − F⟩ = 2.10 Å

**Li(2) polyhedron [6]**

| Li(2) | (F6) | F(13) | F(4) | F(18) | F(11) | F(4) |
|---|---|---|---|---|---|---|
| F(6) | **1.89(1)** | 3.82(1) | 2.99(1) | 2.82(1) | 2.90(1) | 3.08(1) |
| F(13) | 167.6(5) | **1.94(1)** | 2.87(1) | 2.74(1) | 2.86(1) | 3.06(1) |
| F(4) | 94.6(4) | 92.2(5) | **2.02(1)** | 3.46(1) | 3.97(1) | 2.52(1) |
| F(18) | 88.4(5) | 84.1(4) | 175.0(5) | **2.14(1)** | 3.64(1) | 4.42(1) |
| F(11) | 88.1(4) | 85.5(4) | 64.6(3) | 111.6(4) | **2.26(1)** | 2.43(1) |
| F(4) | 99.6(5) | 92.5(4) | 71.3(3) | 112.2(5) | 135.7(6) | **2.28(1)** |

⟨Li(2) − F⟩ = 2.09 Å

TABLE 7—*Continued*

| | | | Li(3) polyhedron [6] | | | |
|---|---|---|---|---|---|---|
| Li(3) | F(19) | F(17) | F(7) | F(8) | F(18) | F(2) |
| F(19) | **1.89(1)** | 2.84(1) | 2.67(1) | 4.08(1) | 3.10(1) | 3.12(1) |
| F(17) | 96.8(4) | **1.91(1)** | 3.83(1) | 2.83(1) | 2.97(1) | 2.96(1) |
| F(7) | 88.6(5) | 170.5(6) | **1.93(1)** | 2.99(1) | 3.13(1) | 2.91(1) |
| F(8) | 163.2(5) | 85.8(4) | 91.3(4) | **2.24(1)** | 2.47(1) | 3.60(1) |
| F(18) | 96.6(4) | 90.9(4) | 96.2(3) | 66.8(2) | **2.25(1)** | 4.60(1) |
| F(2) | 93.7(3) | 87.2(3) | 84.7(3) | 103.0(4) | 169.7(5) | **2.36(1)** |
| | | | ⟨Li(3) − F⟩ = 2.10 Å | | | |

| | | | |
|---|---|---|---|
| Zr(1)–Zr(1) | 3.652(1) | Zr(3)–Zr(4) | 3.596(1) |
| Zr(1)–Zr(2) | 4.184(1) | Zr(4)–Zr(4) | 3.592(1) |
| Zr(1)–Zr(3) | 4.164(1) | Li(1)–Li(3) | 3.71(1) |
| Zr(1)–Zr(3) | 4.159(1) | Li(2)–Li(2) | 3.50(1) |
| Zr(2)–Zr(2) | 3.581(1) | Li(2)–Li(3) | 3.75(1) |
| Zr(2)–Zr(3) | 4.133(1) | | |

pound but did not account for the $Li_4ZrF_8$ fluoride. At about the same time, Korenev *et al.* (2) gave a different version of this $LiF–ZrF_4$ system, showing the $Li_4ZrF_8$ compound and a metastable one corresponding to the $LiF : ZrF_4$ ratio of 1 : 4, leading to the $LiZr_4F_{17}$ formula in addition to that of $Li_3ZrF_7$ and $Li_2ZrF_6$. However they did not mention any compound for the $LiF : ZrF_4$ ratio of 3 : 4. They also concluded that $Li_3ZrF_7$ is dimorphic but gave a temperature of transition very different of that reported by Thoma *et al.*

In light of the structure refinement carried out on $Li_4ZrF_8$ that confirms the existence of such a compound, it appears that all *d* spacings reported in the ASTM card No. 18-760 related to the $\beta$ form of $Li_3ZrF_7$ are included in the X-ray powder pattern of $Li_4ZrF_8$ given in Table 9. This suggests that $Li_3ZrF_7$ is not dimorphic and all that has been reported as being the $\beta$ form of this compound is nothing other than the $Li_4ZrF_8$ compound. A careful examination of the DTA experimental results shows that an invariant of temperature starting on LiF leads to the

TABLE 8
**Valence Bond Analysis[a] for $Li_3Zr_4F_{19}$**

| Atoms | Cations environment and contributions | | | | | | $\Sigma v_{ji}$ | $v_{th}$ |
|---|---|---|---|---|---|---|---|---|
| F(1) | Zr(1) | 0.438 | Zr(1) | 0.455 | Li(1) | 0.105 | 1.00 | 1 |
| F(2) | Zr(1) | 0.715 | Li(1) | 0.133 | Li(3) | 0.067 | 0.91 | 1 |
| F(3) | Zr(4) | 0.422 | Zr(4) | 0.473 | Li(1) | 0.113 | 1.01 | 1 |
| F(4) | Zr(3) | 0.757 | Li(2) | 0.166 | Li(2) | 0.083 | 1.01 | 1 |
| F(5) | Zr(3) | 0.488 | Zr(4) | 0.415 | Li(1) | 0.099 | 1.00 | 1 |
| F(6) | Zr(2) | 0.747 | Li(2) | 0.236 | | | 0.98 | 1 |
| F(7) | Zr(4) | 0.776 | Li(3) | 0.211 | | | 0.99 | 1 |
| F(8) | Zr(2) | 0.462 | Zr(2) | 0.470 | Li(3) | 0.093 | 1.02 | 1 |
| F(9) | Zr(4) | 0.707 | Li(1) | 0.224 | | | 0.93 | 1 |
| F(10) | Zr(1) | 0.540 | Zr(3) | 0.523 | | | 1.06 | 1 |
| F(11) | Zr(3) | 0.457 | Zr(4) | 0.483 | Li(2) | 0.088 | 1.03 | 1 |
| F(12) | Zr(1) | 0.504 | Zr(3) | 0.511 | | | 1.01 | 1 |
| F(13) | Zr(3) | 0.854 | Li(2) | 0.206 | | | 1.06 | 1 |
| F(14) | Zr(1) | 0.826 | Li(1) | 0.185 | | | 1.01 | 1 |
| F(15) | Zr(2) | 0.529 | Zr(3) | 0.562 | | | 1.09 | 1 |
| F(16) | Zr(1) | 0.589 | Zr(2) | 0.426 | | | 1.01 | 1 |
| F(17) | Zr(2) | 0.769 | Li(3) | 0.228 | | | 1.00 | 1 |
| F(18) | Zr(2) | 0.708 | Li(2) | 0.122 | Li(3) | 0.089 | 0.92 | 1 |
| F(19) | Zr(4) | 0.791 | Li(3) | 0.239 | | | 1.03 | 1 |

[a] The expression $v_{ij} = \exp[(R_{ij} - d_{ij})/b]$ taken from Ref. (11) was used with $b = 0.37$, $R_{ij} = 1.854$ for $Zr^{4+}$, and $R_{ij} = 1.360$ for $Li^+$.

TABLE 9
**X-Ray Powder Pattern of $Li_4ZrF_8$**

| $d_{exp}$ (Å) | $d_{calc}$ (Å) | *h k l* | $I/I_0$ |
|---|---|---|---|
| 4.89 | 4.88 | 0 1 1 | 100 |
| 4.82 | 4.81 | 0 2 0 | 36 |
| 4.36 | 4.35 | 1 1 1 | 59 |
| 4.307 | 4.301 | 1 2 0 | 64 |
| 3.668 | 3.668 | 0 2 1 | 30 |
| 3.431 | 3.427 | 1 2 1 | 16 |
| 2.916 | 2.914 | 2 2 1 | 22 |
| 2.789 | 2.792 | 0 3 1 | 11 |
| 2.721 | 2.719 | 0 1 2 | 6 |
| 2.673 | 2.673 | 3 1 1 | 14 |
| 2.619 | 2.617 | 1 1 2 | 4 |
| 2.409 | 2.410 | 3 2 1 | 9 |
| 2.331 | 2.328 | 4 1 0 | 4 |
| 2.150 | 2.151 | 2 4 0 | 31 |
| 2.102 | 2.103 | 3 3 1 | 6 |
| 2.072 | 2.072 | 3 1 2 | 51 |
| 2.011 | 2.011 | 2 4 1 | 8 |
| 1.819 | 1.819 | 4 3 1 | 17 |
| 1.788 | 1.787 | 2 5 0 | 7 |
| 1.758 | 1.758 | 2 0 3 | 3 |
| 1.730 | 1.730 | 2 1 3 | 3 |
| 1.711 | 1.711 | 4 2 2 | 3 |
| 1.700 | 1.700 | 4 4 0 | 10 |
| 1.651 | 1.651 | 2 2 3 | 4 |

**TABLE 10**
**X-Ray Powder Pattern of $Li_3Zr_4F_{19}$**

| $d_{exp}$ (Å) | $d_{calc}$ (Å) | $h\ k\ l$ | $I/I_0$ |
|---|---|---|---|
| 6.68 | 6.68 | 0 1 1 | 5 |
| 6.09 | 6.08 | 0 $\bar{1}$ 2 | 31 |
| 5.228 | 5.230 | 1 0 0 | 43 |
| 4.880 | 4.880 | 1 $\bar{1}$ 1 | 18 |
| 4.632 | 4.635 | 0 $\bar{2}$ 2 | 28 |
| 4.300 | 4.290 | 1 1 $\bar{1}$ | 9 |
| 4.214 | 4.215 | 0 $\bar{1}$ 3 | 29 |
| 4.008 | 4.005 | 0 0 3 | 14 |
| 3.895 | 3.891 | 1 1 $\bar{2}$ | 100 |
| 3.755 | 3.756 | $\bar{1}$ 2 1 | 20 |
| 3.498 | 3.501 | 0 $\bar{3}$ 1 | 18 |
| 3.338 | 3.342 | 0 2 2 | 67 |
| 3.292 | 3.296 | 1 $\bar{3}$ 1 | 60 |
| 3.263 | 3.257 | 1 $\bar{1}$ 3 | 54 |
| 3.172 | 3.171 | 0 $\bar{1}$ 4 | 14 |
| 3.093 | 3.090 | 0 $\bar{3}$ 3 | 4 |
| 3.003 | 3.004 | 0 0 4 | 4 |
| 2.851 | 2.855 | 1 $\bar{3}$ 3 | 2 |
| 2.747 | 2.748 | $\bar{1}$ 0 4 | 2 |
| 2.651 | 2.650 | 0 1 4 | 4 |
| 2.618 | 2.616 | 0 $\bar{4}$ 2 | 6 |
| 2.578 | 2.578 | 2 $\bar{2}$ 1 | 6 |
| | 2.578 | 1 $\bar{4}$ 2 | |
| 2.526 | 2.525 | $\bar{2}$ 2 1 | 11 |
| 2.439 | 2.440 | 2 $\bar{2}$ 2 | 6 |
| | 2.439 | 2 $\bar{1}$ 2 | |
| 2.368 | 2.368 | 2 1 $\bar{2}$ | 7 |
| 2.330 | 2.330 | 1 3 1 | 3 |
| | 2.329 | 1 1 5 | |
| 2.303 | 2.303 | 1 3 $\bar{4}$ | 10 |
| 2.269 | 2.269 | 0 2 4 | 5 |
| 2.248 | 2.247 | 1 $\bar{4}$ 4 | 14 |
| 2.229 | 2.228 | 0 3 3 | 10 |
| 2.187 | 2.188 | 1 $\bar{3}$ 5 | 6 |
| 2.157 | 2.157 | 1 4 $\bar{2}$ | 6 |
| | 2.157 | 2 2 $\bar{1}$ | |
| 2.076 | 2.076 | 1 5 3 | 12 |
| | 2.075 | 0 4 2 | |

composition 75 mole% of LiF, whereas another one slightly lower in temperature appears between 80 and 66.67 mole% of LiF (Fig. 5). This supports the conclusion that the first one may be assigned to the decomposition of $Li_4ZrF_8$ in the solid state while the second one is relative to the thermal decomposition of the metastable $Li_3ZrF_7$ fluoride on cooling. It should also be noticed that this conclusion does not disagree with the comment reported in the ASTM card No. 18-760, according to which the assumed $\beta$ form of $Li_3ZrF_7$ was stable in a very narrow interval of temperature (470–475°C) since the two-phase region including $Li_4ZrF_8$ and $Li_3ZrF_7$ appears in this temperature range. With the crystal structure determination of the $Li_3Zr_4F_{19}$ compound now supplied, the X-ray powder pattern of which is given in Table 10, we confirm the high $ZrF_4$ content side of the phase diagram reported by Thoma *et al.* We did not succeed in attempting to characterize a well-defined combination for the LiF : $ZrF_4$ ratio of 1 : 4. For the higher $ZrF_4$ content compositions heated in sealed platinum tubes and quenched in cold water from temperatures higher than 580°C, the $\alpha$ form of $ZrF_4$ (15) has been identified in the X-ray powder patterns of the samples. The phase equilibrium diagram for this system redrawn to conform with our additional results is shown in Fig. 5. The main characteristics of this diagram are gathered in Table 1.

## REFERENCES


1. R. E. Thoma, H. Insley, H. A. Friedman, and G. M. Herbert, *J. Chem. Eng. Data* **10**(3), 219 (1965).
2. Y. M. Korenev, A. V. Novoselova, K. K. Glinskii, and U. V. Shornikov, *Izv. Akad. Nauk SSSR Neorg. Mater.* **1**(2), 201 (1965); (Engl. Transl.) *Inorg. Mater.* **1**(2), 184 (1965).
3. H. W. Sun, B. Tanguy, J. M. Reau, and J. Portier, *J. Solid State Chem.* **63,** 191 (1986).
4. M. Poulain, M. Poulain, J. M. Reau, and J. Portier, *Mater. Res. Bull.* **10,** 243 (1975).
5. D. Leroy, J. Lucas, M. Poulain, and D. Ravaine, *Mater. Res. Bull.* **13,** 1125 (1978).
6. G. V. Chandrashekhar and M. W. Shafer, *Mater. Res. Bull.* **15,** 22 (1980).
7. Y. Kawamoto, R, Kanno, R. Yokota, M. Takahashi, S. Tanabe, and K. Hirao, *J. Solid State Chem.* **103**(2), 334 (1993).
8. M. El-Ghozzi, D. Avignant, and J. C. Cousseins, *Eur. J. Solid State Inorg. Chem.* **29,** 981 (1992).
9. G. Brunton, *J. Inorg. Nucl. Chem.* **29,** 1631 (1967).
10. G. Brunton, *Acta Crystallogr. B* **29,** 2294 (1973).
11. N. E. Brese and M. O'Keeffe, *Acta Crystallogr. B* **47,** 192 (1991).
12. "International Tables for X-ray Crystallography," Vol. IV. Kynoch Press, Birmingham, 1968.
13. B. A. Frenz, in "Computing in Crystallography" (H. Shenk, R. Olthof-Hazekamp, H. Van Koningveld, and G. C. Bassi, Eds.). Delft Univ. Press, Delft, The Netherlands (1982).
14. R. D. Shannon, *Acta Crystallogr. A* **32,** 751 (1976).
15. R. Papiernik, D. Mercurio, and B. Frit, *Acta Crystallogr. B* **38,** 2347 (1982).